Biomedical Optics EXPRESS

Hydrogenated amorphous silicon nitride photonic crystals for improved-performance surface electromagnetic wave biosensors

Alberto Sinibaldi,[1] Emiliano Descrovi,[2] Fabrizio Giorgis,[2] Lorenzo Dominici,[1] Mirko Ballarini,[2] Pietro Mandracci,[2] Norbert Danz,[3] and Francesco Michelotti[1,*]

[1] *Dipartimento di Scienze di Base ed Applicate per l'Ingegneria, SAPIENZA Università di Roma, Via A. Scarpa 16, 00161 Roma, Italy*

[2]*Dipartimento di Scienza Applicata e Tecnologia, Politecnico di Torino, C.so Duca degli Abruzzi 24, 10129 Torino, Italy*

[3]*Fraunhofer Institute for Applied Optics and Precision Engineering IOF, Albert-Einstein-Str. 7, 07745 Jena, Germany*

**francesco.michelotti@uniroma1.it*

Abstract: We exploit the properties of surface electromagnetic waves propagating at the surface of finite one dimensional photonic crystals to improve the performance of optical biosensors with respect to the standard surface plasmon resonance approach. We demonstrate that the hydrogenated amorphous silicon nitride technology is a versatile platform for fabricating one dimensional photonic crystals with any desirable design and operating in a wide wavelength range, from the visible to the near infrared. We prepared sensors based on photonic crystals sustaining either guided modes or surface electromagnetic waves, also known as Bloch surface waves. We carried out for the first time a direct experimental comparison of their sensitivity and figure of merit with surface plasmon polaritons on metal layers, by making use of a commercial surface plasmon resonance instrument that was slightly adapted for the experiments. Our measurements demonstrate that the Bloch surface waves on silicon nitride photonic crystals outperform surface plasmon polaritons by a factor 1.3 in terms of figure of merit.

OCIS codes: (240.6690) Surface waves; (230.5298) Photonic crystals; (130.6010) Sensors; (160.5293) Photonic bandgap materials; (170.4580) Optical diagnostics for medicine.

References and Links

1. B. Liedberg, C. Nylander, and I. Lundström, "Biosensing with surface plasmon resonance--how it all started," Biosens. Bioelectron. **10**(8), i–ix (1995).
2. M. Piliarik and J. Homola, "Surface plasmon resonance (SPR) sensors: approaching their limits?" Opt. Express **17**(19), 16505–16517 (2009).
3. M. Shinn and W. M. Robertson, "Surface plasmon-like sensor based on surface electromagnetic waves in a photonic band-gap material," Sens. Act. B Chem. **105**(2), 360–364 (2005).
4. P. Rivolo, F. Michelotti, F. Frascella, G. Digregorio, P. Mandracci, L. Dominici, F. Giorgis, and E. Descrovi, "Real time secondary antibody detection by means of silicon-based multilayers sustaining Bloch surface waves," Sens. Act. B Chem. **161**(1), 1046–1052 (2012).
5. Y. Guo, J. Y. Ye, C. Divin, B. Huang, T. P. Thomas, J. R. Baker, Jr., and T. B. Norris, "Real-time biomolecular binding detection using a sensitive photonic crystal biosensor," Anal. Chem. **82**(12), 5211–5218 (2010).
6. P. Yeh, A. Yariv, and C.-S. Hong, "Electromagnetic propagation in periodic stratified media. I. General theory," J. Opt. Soc. Am. **67**(4), 423–438 (1977).
7. J. Homola, *Surface Plasmon Resonance Based Sensors* (Springer-Verlag, Berlin, 2006).
8. C. Summonte, R. Rizzoli, M. Bianconi, A. Desalvo, D. Iencinella, and F. Giorgis, "Wide band-gap silicon-carbon alloys deposited by very high frequency plasma enhanced chemical vapor depositions," J. Appl. Phys. **96**(7), 3987–3997 (2004).
9. F. Demichelis, F. Giorgis, and C. F. Pirri, "Compositional and structural analysis of hydrogenated amorphous silicon-nitrogen alloys prepared by plasma-enhanced chemical vapour deposition," Philos. Mag. B **74**(2), 155–168 (1996).

#171841 - $15.00 USD Received 3 Jul 2012; rev. 20 Jul 2012; accepted 24 Jul 2012; published 6 Sep 2012

10. S. H. Baker, W. E. Spear, and R. A. G. Gibson, "Electronic and optical properties of a-$Si_{1-x}C_x$ films prepared from a H_2-diluted mixture of SiH_4 and CH_4," Philos. Mag. B **62**(2), 213–223 (1990).
11. C. Ricciardi, V. Ballarini, M. Galli, M. Liscidini, L. C. Andreani, M. Losurdo, G. Bruno, S. Lettieri, F. Gesuele, P. Maddalena, and F. Giorgis, "Amorphous silicon nitride: a suitable alloy for optical multilayered structures," J. Non-Cryst. Solids **352**(9-20), 1294–1297 (2006).
12. F. Giorgis, C. F. Pirri, C. Vinegoni, and L. Pavesi, "Luminescence processes in amorphous hydrogenated silicon-nitride nanometric multilayers," Phys. Rev. B **60**(16), 11572–11576 (1999).
13. S. Lettieri, S. Di Finizio, P. Maddalena, V. Ballarini, and F. Giorgis, "Second-harmonic generation in amorphous silicon nitride microcavities," Appl. Phys. Lett. **81**(25), 4706–4708 (2002).
14. E. Descrovi, F. Giorgis, L. Dominici, and F. Michelotti, "Experimental observation of optical bandgaps for surface electromagnetic waves in a periodically corrugated one-dimensional silicon nitride photonic crystal," Opt. Lett. **33**(3), 243–245 (2008).
15. R. Martins, P. Baptista, L. Raniero, G. Doria, L. Silva, R. Franco, and E. Fortunato, "Amorphous/nano-crystalline silicon biosensor for the specific identification of unamplified nucleic acid sequences using gold nanoparticle probes," Appl. Phys. Lett. **90**(2), 023903 (2007).
16. M. Ballarini, F. Frascella, N. De Leo, S. Ricciardi, P. Rivolo, P. Mandracci, E. Enrico, F. Giorgis, F. Michelotti, and E. Descrovi, "A polymer-based functional pattern on one-dimensional photonic crystals for photon sorting of fluorescence radiation," Opt. Express **20**(6), 6703–6711 (2012).
17. M. Ballarini, F. Frascella, E. Enrico, P. Mandracci, N. De Leo, F. Michelotti, F. Giorgis, and E. Descrovi, "Bloch surface waves-controlled fluorescence emission: coupling into nanometer-sized polymeric waveguides," Appl. Phys. Lett. **100**(6), 063305 (2012).
18. N. Danz, A. Kick, F. Sonntag, S. Schmieder, B. Höfer, U. Klotzbach, and M. Mertig, "Surface plasmon resonance platform technology for multi parameter analyses on polymer chips," Eng. Life Sci. **11**(6), 566–572 (2011).
19. A. Sinibaldi, N. Danz, E. Descrovi, P. Munzert, U. Schulz, F. Sonntag, L. Dominici, and F. Michelotti, "Direct comparison of the performance of Bloch surface wave and surface plasmon polariton sensors," Sens. Act. B Chem. (to be published).
20. J. Homola, S. S. Yee, and G. Gauglitz, "Surface plasmon resonance sensors: review," Sens. Act. B Chem. **54**(1-2), 3–15 (1999).
21. R. C. Weast, *CRC Handbook of Chemistry and Physics*, 55th ed. (CRC, Cleveland, 1974).
22. A. Shalabney and I. Abdulhalim, "Figure-of-merit enhancement of surface plasmon resonance sensors in the spectral interrogation," Opt. Lett. **37**(7), 1175–1177 (2012).

1. Introduction

In the wide range of bio-sensing techniques, surface plasmon resonance (SPR) optical biosensors [1] have become a mature technology for simple and fast label free bio-detection [2]. Due their surface-bound nature, surface plasmon polaritons (SPP) are used to sense the refractive index changes in a very narrow region in close proximity of the sensor surface, mainly in real-time conditions. Unfortunately some intrinsic properties of SPP limit a further refinement of SPR sensitivity. The most critical point is that SPP dispersion is strictly determined by the properties of a limited number of suitable metals and cannot be arbitrarily tuned. This point also includes large absorption losses at optical frequencies which result in SPP damping and resonance broadening. A possible solution [3–5] to improve the performances of optical biosensors is to exploit another kind of surface localized electromagnetic waves: e.g. Bloch Surface Waves (BSW) on dielectric multilayers. Such electromagnetic modes can propagate at the interface between a finite one-dimensional photonic crystal (1DPC) and a homogeneous external medium [6]. Their dispersion can be designed at any desired operation wavelength by properly tailoring the 1DPC, in terms of the refractive index and thickness of the layers. Dielectrics exhibit much lower extinction coefficients than metals and the BSW resonances (BSWR) appear much narrower than the SPR [7], with an expected increase of sensor performances.

We explore the viability of the well-established amorphous silicon thin film technology for the fabrication of 1DPC supporting surface bound waves for sensing applications. Amorphous silicon based alloys such as hydrogenated silicon nitride (a-Si_xN_y:H), silicon carbide (a-Si_xC_y:H) and silicon oxide (a-Si_xO_y:H) can be easily grown by r.f. plasma-enhanced chemical vapor deposition (PE-CVD) on large area with an excellent control of the compositional homogeneity and thickness at nanometer scale. The average stoichiometry of the alloys can be fixed through the suitable choice of the gas feedstock composition, allowing a direct control of the thin films optical response in terms of absorption and refractive index [8–10]

#171841 - $15.00 USD Received 3 Jul 2012; rev. 20 Jul 2012; accepted 24 Jul 2012; published 6 Sep 2012

Among the amorphous silicon alloys cited above, a-Si_xN_y:H shows a tunable refractive index with values ranging from 1.7 (for a-Si_3N_4:H) and 3.5 (pure a-Si:H) and optical gap variable within 1.9 (pure a-Si:H) and 5 eV (a-Si_3N_4:H) [9,11]. In detail, the composition of the a-Si_xN_y:H layers can be controlled by operating on the ammonia fraction in a SiH_4 + NH_3 plasma, allowing the fabrication of high quality periodic stratified structures alternating Si-rich and N-rich a-Si_xN_y:H layers. Several a-Si_xN_y:H based multilayer structures were proposed for the realization of multi-quantum-well light emitting systems [12], Bragg reflectors, Fabry-Perot microcavities [13] and 1DPC sustaining BSW [14]. The use of a-Si_xN_y:H for unamplified nucleic acid sequences biosensors was also reported [15].

A stratified structure made of Si_xN_y:H with variable average stoichiometry can benefit of a wide range of refractive index tunability, allowing the versatile use of silicon nitride alloys in the fabrication of 1DPC with suitable refractive index contrast and transparency, operating with BSW either in the near infrared [14] or in the visible spectral range [16,17].

We report experimental results obtained for three different optical biosensors: a standard gold SPP chip and two chips based on a-Si_xN_y:H 1DPC, the first one supporting a guided mode (GM), and the second one a Bloch surface mode (BSW). Such results permit to make a direct comparison of the sensing performances of GM and BSW with respect to SPP.

2. Materials and methods

All optical measurements reported here were obtained by means of a SPR instrument, developed by one of the authors [18]. In the standard configuration, the instrument makes use of disposable plastic chips with integrated coupling optics, on which a 45 nm thick gold film is directly deposited by sputtering. Here we used adaptor plastic chips which were thinned and topped with a cover slip glued to their surface. Such adaptor chips could accommodate the samples deposited on standard 170 µm thick cover slips on their top and operate under comparable conditions for both SPP and BSW. The samples were coupled to the adaptor chips by means of contact oil (refractive index 1.518).

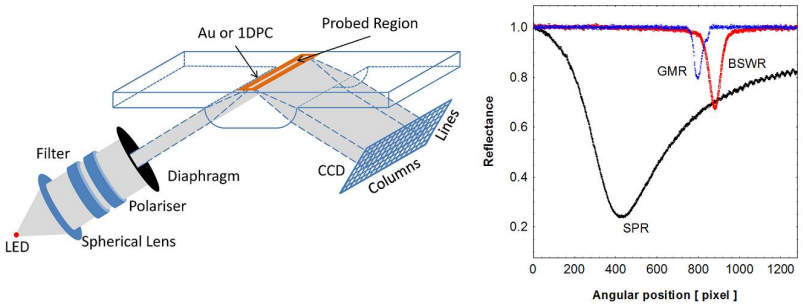

Fig. 1. Left, sketch of the optics of the SPR platform used in the experiments. Right, angular reflectance curves obtained experimentally with the SPR platform. Each measurement is the average of 15 neighboring columns. The x angular scale is given in pixels of the CCD detector; data are normalized to the reflectance measured in air environment. (SPR) 45nm gold layer, (GMR) 1DPC sustaining a guided mode, (BSWR) 1DPC sustaining a Bloch surface wave.

In Fig. 1 (left) we show a sketch of the optical module of the SPR platform. The beam from a light emitting diode (LED) is collimated by means of a spherical lens. The bandwidth is reduced by means of a 2.5 nm FWHM interferential filter peaked at λ = 804 nm (Chroma) and its polarization is defined by means of a thin film polarizer (Codixx AG) which can be rotated to ensure either TM or TE illumination. The beam is then focused by the input cylindrical diopter to an elongated spot onto the surface of the sensor. The incidence angle is 66 deg and the angular aperture of the focused beam is ± 2 deg. The reflected beam is collimated by the output diopter and sent to a charge coupled device (CCD). The intensity distribution along the columns of the CCD corresponds to the one dimensional Fourier transform of the reflected beam. This sensing approach provides an angular resolved reflectivity measurement of horizontal stripes parallel to the surface waves propagation

#171841 - $15.00 USD Received 3 Jul 2012; rev. 20 Jul 2012; accepted 24 Jul 2012; published 6 Sep 2012

direction by selecting the appropriate range of CCD rows corresponding to the spatial areas to be analyzed. We used either 1DPC or single gold layers deposited on standard cover slips. When conducting the comparison, SPR and BSWR measurements have been performed with the same set-up, the only difference consisting in the polarization of the illumination.

Two types of 1DPCs based on a-Si_xN_y:H were designed, showing a resonance in the sensitive window of the SPR platform, aiming to explore the sensing capabilities of a GM and a BSW, respectively. The 1DPC were then fabricated by 13.56 MHz PE-CVD on 170 μm thick glass cover slides (25x64mm). The refractive indices and thicknesses of single test layers were characterized by reflectance spectroscopy and their values used in the numerical simulations carried out to design the 1DPC.

The first 1DPC was designed to support a GM and it is constituted by a 6 periods stack of high (a-$Si_{0.62}N_{0.38}$:H, n_H = 2.47 at 804 nm) and low (a:SiO_2:H, n_L = 1.48 at 804 nm) refractive index layers, having thickness d_H = 175 nm and d_L = 300 nm, respectively. The second 1DPC was designed to support the BSW and it is constituted by a 6 periods stack of high (a-$Si_{0.62}N_{0.38}$:H, n_H = 2.47 at 804 nm) and low (a-Si_3N_4:H, n_L = 1.76 at 804nm) refractive index layers, with d_H = 123 nm and d_L = 185 nm, respectively. The final stoichiometry and the optical properties of the layers were determined by choosing of the gas feedstock composition in the PE-CVD process [9,11]. In detail, the silicon nitride layers were deposited in SiH_4 + NH_3 plasmas with ammonia percentage $[NH_3]/[SiH_4 + NH_3]$ = 53.3% for the Si-rich alloy and 94.7% for the stoichiometric one. The deposition conditions were: r.f. power density 208 W/m^2, pressure 450 mTorr, total gas flow rate 75 sccm, substrate temperature 220°C. On the other hand, the stoichiometric silicon oxide layers were deposited in SiH_4 + CO_2 + H_2 plasmas with CO_2 percentage $[CO_2/(CO_2 + SiH_4)]$ = 97.5% and H_2 percentage $[H_2/(CO_2 + SiH_4 + H_2)]$ = 70.9%. The deposition conditions were: r.f. power density 1042 W/m^2, pressure 600 mTorr, total gas flow rate 141 sccm, substrate temperature 220°C.

The number of the 1DPC periods was chosen in order to optimize the coupling efficiency.

Reference samples supporting SPP were obtained by depositing an 45 nm thick gold layer by means of magnetron sputtering on 170 μm thick glass cover slides, according to the same standard procedure used to produce chips on plastic substrates for the SPR platform.

3. Results

In Fig. 1 (right) we show the experimental measurement of the reflectivity profile along the columns of the CCD camera. Such profiles correspond to the angular spectrum of the reflected radiation along this direction. The angular spectra are given versus camera pixels in the following with an approximate scale of 0.003 deg/pixel. All measurements were carried out in doubly deionized water (ddH_2O), at ambient temperature and in either TM or TE polarization for SPP and BSW, respectively. The measurements were obtained by averaging signals over 15 columns of the CCD in the read out system.

At a first inspection yet, the GMR and BSWR in Fig. 1 look much narrower than the SPR, as expected because of the reduced losses. We found for the full width half maximum W and for the depth D of the resonances the values reported in Table 1, for the three cases. We note that the measured width (depth) of the BSWR is larger (smaller) than that expected from numerical simulations carried out by the transfer matrix method at a single wavelength (804 nm). Such effect is due to the bandwidth of the illumination that is larger than the bandwidth of the BSW resonance and to a slight inhomogeneity of the thickness of the 1DPC layers [19]. We point out that small thickness variations that are weakly affecting standard optical characteristics, such as normal transmittance, might be more critical for the optimal BSW coupling.

With the purpose of evaluating the sensitivity of the chips with respect to perturbations the external medium refractive index, we used glucose solutions with an increasing concentration, ranging from 0.01% to 10% in weight. Measurements were carried out by dropping the solutions directly on the chip surface by means of a pipette and then by measuring the resulting resonance shift. Each drop has been removed from the sensing area by means of an air blow before depositing the next solution droplet. Between two successive measurements

#171841 - $15.00 USD Received 3 Jul 2012; rev. 20 Jul 2012; accepted 24 Jul 2012; published 6 Sep 2012

the surface was washed with ddH_2O to check for returning to zero of the resonance shift and to prevent mixing of the solutions, with uncontrolled changes of the real value of the glucose concentration. The measurements were repeated several times, with the same result within the errors.

Table 1. Parameters extracted from the experimental measurements carried out on 1DPC supporting either GM or BSW and on gold thin films supporting SPP. Parameters are defined in the text.

Sensor Type	W [pixel]	W [deg]	D	S [pixel/%]	S [deg/RIU]	Q	Q/S [RIU/deg]	FOM [RIU^{-1}]
GM	38 ± 1	0.115 ± 0.003	0.22 ± 0.01	4.95 ± 0.05	9.7 ± 0.1	0.08	~0.008	19 ± 2
BSW	58 ± 1	0.175 ± 0.003	0.34 ± 0.01	13.4 ± 0.1	26.3 ± 0.3	0.323	~0.012	52 ± 3
SPP	520 ± 10	1.56 ± 0.03	0.73 + 0.01	40.3 ± 0.4	79.3 ± 0.8	0.678	~0.008	39 ± 2

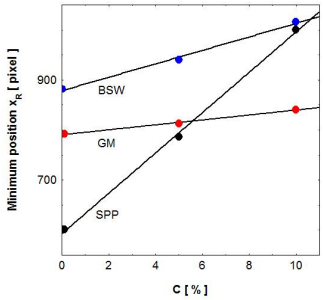

Fig. 2. Positions of the resonances as a function of the glucose concentration in solutions, for both 1DPC (BSW and GM) and SPP based biochips on cover slips. The errors are smaller than the dimension of the symbols. Each point is the result of a 15 min long measurement.

Figure 2 shows the results of the measurements obtained by means of the procedure described above. From collected data we can evaluate the slopes of the fitting lines, corresponding to the sensitivity S [20], for the three sensors (Table 1). We notice that the SPP mode shows the maximum S, whereas for the BSW we obtain a lower value and a minimum S for the GM. As expected, the GM shows a smaller S compared to the two surface bound waves. In order to convert the results in terms of changes of the refractive index of the external medium we used the formula $\Delta n = \beta \cdot C$ for the refractive index change of glucose solutions in ddH_2O, with a coefficient $\beta = 1.527 \cdot 10^{-3}$ RIU/% [21]. Taking into account the conversion factor 0.003 deg/pixel, the sensitivities can then be expressed in terms of the change of the resonance angle as a function of Δn. Such conversion allows one to rewrite S in deg/RIU units (Table 1), allowing a simple comparison with data published by other researchers.

4. Discussion

The different values found for the S of the three types of sensors are due to the different transverse intensity distributions across the sensors themselves. We analyzed the transverse intensity distributions for the GM, BSW and SPP mode respectively, and evaluated numerically the ratio between the power associated to the mode tail in the external medium P_{TAIL} and the total power carried by the mode P_{TOT}. In Fig. 3 we show the transverse intensity distributions for GM, BSW and SPP calculated at $\lambda = 804$ nm by means of a transfer matrix approach. We note that the penetration depth in all cases is almost the same, as the structures were designed to support GM and BSW resonating at the same angle as SPP on gold.

The ratios $Q = P_{TAIL}/P_{TOT}$ found for the three modes are reported in Table 1. For the GM and the SPP the S values scale with the Q value, giving a ratio $Q_{GM}/S_{GM} \sim Q_{SPP}/S_{SPP} \sim 0.008$. However, for the BSW the ratio $Q_{BSW}/S_{BSW} \sim 0.012$ confirms that the BSWR is broadened and the real transverse intensity is bound to the surface to a lesser extent with a decrease of S. We expect that, for a narrower illumination bandwidth the BSW the sensitivity S would be larger

#171841 - $15.00 USD Received 3 Jul 2012; rev. 20 Jul 2012; accepted 24 Jul 2012; published 6 Sep 2012

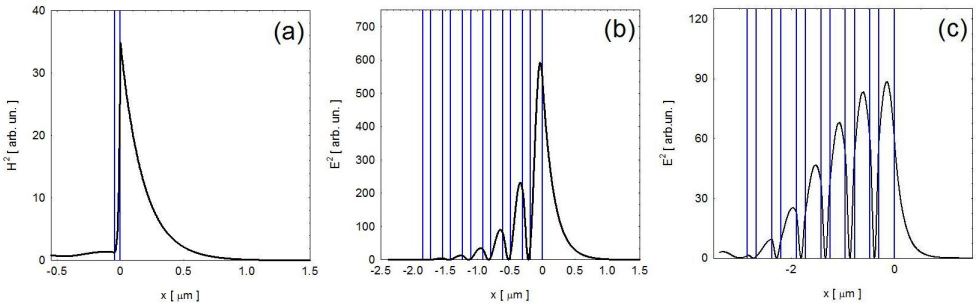

Fig. 3. Square modulus of transverse intensity distributions in the normal direction (x) for (a) SPP, (b) BSW and (c) GM calculated at λ = 804 nm. The zero on the abscissa corresponds to the surface of the sample.

so as to give the same ratio Q_{BSW}/S_{BSW} ~0.008, i.e., would be of the order of S_{BSW} = 40 deg/RIU. Such value would be anyhow lower than that obtained with SPP.

When evaluating the performance of sensors, in view of the determination of their resolution and limit of detection (LoD), we must take into account also the width and the depth of the resonances. Usually researchers operating in the field define a figure of merit as the ratio of the sensitivity to the full width half maximum of the resonances [22]. Here, in order to compare the performance of the sensors, we introduce a composite figure of merit FOM = D·S/W, including the depth D, the sensitivity S and the width W [19]. The FOM for the three types of sensors assume the values that are reported in Table 1.

Therefore, from our comparison measurements we find that, for the particular designs we chose for the 1DPC, we get the ratio FOM_{GM}/FOM_{SPP} = 0.5 indicating that the SPP chips outperform the chips supporting the GM. On the other hand the ratio FOM_{BSW}/FOM_{SPP} = 1.3 demonstrates that we can reach a better performance, and resolution, by using a chip based on a 1DPC supporting a Bloch surface wave instead of a standard chip supporting a SPP.

5. Conclusions

The experimental results shown demonstrate an improvement of the performance of optical biosensors, obtained by using an a-Si_xN_y:H 1DPC supporting a BSW instead of SPP on thin metal layers. We introduced a figure of merit to evaluate the performance in angular resolved reflectivity measurement mode and have shown that sensors based on BSW on a-Si_xN_y:H 1DPC outperform SPR sensors by at least a factor 1.3. A reduction of the limitation imposed by the illumination bandwidth can push, for the design reported here, such a factor up to 2.

We showed the a-Si_xN_y:H technology to be a good platform technology for refractive index tuning of high optical quality layers to be used in 1DPC biosensors.

We point out that BSW on 1DPC, besides improving performance and resolution, can be designed for any range of wavelengths and open the access to regions where SPR, due to limitations introduced by the metals dispersion, cannot operate.

Acknowledgments

This work is partially funded by the SAPIENZA University research program, by Piedmont Regional project CIPE 2008 “PHotonic biOsensors for Early caNcer diagnostICS (PHOENICS),” and by the national project FIRB 2011 “Advanced nanosystems for a new era in molecular oncology (NEWTON).”

#171841 - $15.00 USD Received 3 Jul 2012; rev. 20 Jul 2012; accepted 24 Jul 2012; published 6 Sep 2012